International Journal of Engineering Research and Technology. ISSN 0974-3154, Volume 12, Number 12 (2019), pp. 2185-2190

Influence of Initial Conditions on Motion Behaviors of Robot Arms

Do Trung Hai, Nguyen Hong Quang*

Department of Automation, Thai Nguyen University of Technology, Viet Nam.

**(Corresponding Author. ORCID: 0000-0002-0433-3094)*

Abstract

Closed loop multibody systems are strong nonlinear systems. In strong nonlinear systems with the same system parameters, there may be many different solutions depending on the initial conditions. The mechanism is the typical form of closed loop multibody systems. The determination of the rotational movement of the driving section of the mechanism is an interesting problem in machine dynamics. In this paper, the equations of motion of closed loop multibody systems are formulated as Differential Algebraic Equations (DAE). Then the Lagrangian multiplier partitioning method is used to transform the differential - algebraic equations into ordinary differential equations. In order to study the dependence of the motion of the mechanism on the initial conditions, we solve the system of differential equations for motion of the mechanism with different initial conditions. Numerical simulation results using MATLAB® software show the influence of initial conditions on the rotational motion of the driving section of the robotic mechanism.

Keywords: Lagrangian equations with multipliers, strong nonlinear systems, Differential Algebraic Equations, Baumgarte stabilization method, rotational motion.

I. INTRODUCTION

Dynamics of closed loop multibody systems is a problem that is of great interest. In order to set the equations of motion of these mechanical models, Lagrangian equations with multipliers, Newton-Euler equations, and Kane equations with multipliers [1-6] are often used. If we choose the number of extrapolating coordinates to determine the position of the mechanical system which is greater than the number of degrees of freedom of the system, we get the system of differential-algebraic equations describing the movement of the mechanism in the explicit form. To solve this type of motion equation system, there are currently three options:

- Direct integral of the system of differential- algebraic equations.
- Convert the system of differential- algebraic equations to the system of ordinary differential equations with the number of extrapolating coordinates greater than the number of degrees of freedom of the system. Then integrate the system of differential equations received.
- Convert the system of differential- algebraic equations to the system of ordinary differential equations with the number of extrapolating coordinates equal to the number of degrees of freedom of the system. Then integrate the system of differential equations received.

In this paper, we apply the Lagrangian equations with multipliers to set the equation of motion of the slider-crank mechanism, then use the second method to solve the system of the equations of motion of the mechanism. The differential equations describing the motion of the mechanism are strong nonlinear differential equations.

As known in [7-8], the solutions of a strong nonlinear system has many different properties from those of the linear systems and the weak nonlinear systems. For example, the solutions of strong nonlinear systems can be chaotic solutions, sensitively depending on the initial conditions. Studying the dependence of the rotational movement of the mechanism on the initial conditions is the most important part of the paper. Studies that simulate the number of motions of the mechanism with different initial conditions have shown some new nonlinear effects of the motion of the mechanism.

II. THEORY OF DYNAMICS OF CLOSED LOOP MULTIBODY SYSTEMS

This section reiterates some of the necessary knowledge of dynamics of closed loop multibody systems. Consider holonom closed loop multibody system f with variants. The position of the system is determined by the extrapolating coordinates n:

$$\mathbf{s} = \left[s_1, s_2, ..., s_n\right]^T \tag{1}$$

Which has the independent extrapolation coordinate f:

$$\mathbf{q} = [q_1, q_2, ..., q_f]^T \tag{2}$$

and the independent extrapolation coordinate r:

$$\mathbf{z} = \left[z_1 \;\; z_2 \;\; ... \;\; z_r\right]^T \tag{3}$$

So we have the system $n = f + r$ (4)

Using Lagrangian equations with multipliers, the differential - algebraic equations describing the motion of the system have the form [1]:

$$\mathbf{M}(\mathbf{s})\ddot{\mathbf{s}} + \mathbf{C}(\mathbf{s}, \dot{\mathbf{s}})\dot{\mathbf{s}} + \mathbf{g}(\mathbf{s}) = \boldsymbol{\tau}(t) - \boldsymbol{\Phi}_s^T(\mathbf{s})\boldsymbol{\lambda} \tag{5}$$

$$\mathbf{f}(\mathbf{s}) = \mathbf{0} \tag{6}$$

Where $\mathbf{M}(\mathbf{s})$ is the extrapolation mass matrix of the system, $\boldsymbol{\tau}(t)$ is the extrapolation force vector corresponding to the operating forces without fulcrum, $\boldsymbol{\lambda} = \left[\lambda_1, \lambda_2, ..., \lambda_r\right]^T$ is a Lagrangian multipliers vector, $\mathbf{f} = \left[f_1,\ f_2, ..., f_r\right]^T = \mathbf{0}$ are binding conditions, $\boldsymbol{\Phi}_s$ is the Jacobi matrix of $\mathbf{f}$ of size $r \times n$, $\mathbf{C}(\mathbf{s}, \dot{\mathbf{s}})$ is the centrifugal inertia matrix and Coriolis, **g(s)** is the extrapolation force vector corresponding to the operating forces with fulcrum.

To conveniently convert equations (5) and (6), we add a symbol:

$$\mathbf{p}_1(\mathbf{s}, \dot{\mathbf{s}}, t) = \boldsymbol{\tau}(t) - \mathbf{C}(\mathbf{s}, \dot{\mathbf{s}})\dot{\mathbf{s}} - \mathbf{g}(\mathbf{s}),\ \mathbf{p}_1(\dot{\mathbf{s}}, \mathbf{s}, t) \in \mathbb{R}^n \tag{7}$$

Equation (4) now takes the form:

$$\mathbf{M}(\mathbf{s})\ddot{\mathbf{s}} + \boldsymbol{\Phi}_s^T\ \mathbf{s}\ \boldsymbol{\lambda} = \mathbf{p}_1(\mathbf{s}, \dot{\mathbf{s}}, t) \tag{8}$$

Double derivative equations (6) we obtain equations:

$$\dot{\mathbf{f}}(\mathbf{s}) = \frac{\partial \mathbf{f}}{\partial \mathbf{s}}\dot{\mathbf{s}} = \boldsymbol{\Phi}_s(\mathbf{s})\dot{\mathbf{s}} = \mathbf{0} \tag{9}$$

$$\ddot{\mathbf{f}}(\mathbf{s}) = \boldsymbol{\Phi}_s(\mathbf{s})\ddot{\mathbf{s}} + \dot{\boldsymbol{\Phi}}_s(\mathbf{s})\dot{\mathbf{s}} = \mathbf{0} \tag{10}$$

Where $\boldsymbol{\Phi}_s \in \mathbb{R}^{r \times n}$. From (10) we have:

$$\boldsymbol{\Phi}_s\ddot{\mathbf{s}} = -\dot{\boldsymbol{\Phi}}_s(\mathbf{s})\dot{\mathbf{s}} = \mathbf{p}_2(\mathbf{s}, \dot{\mathbf{s}}) \tag{11}$$

Equations (8) and (11) can be rewritten as a matrix:

$$\begin{bmatrix} \mathbf{M} & \boldsymbol{\Phi}_s^T \\ \boldsymbol{\Phi}_s & \mathbf{0} \end{bmatrix}\begin{bmatrix} \ddot{\mathbf{s}} \\ \boldsymbol{\lambda} \end{bmatrix} = \begin{bmatrix} \mathbf{p}_1 \\ \mathbf{p}_2 \end{bmatrix} \tag{12}$$

When using numerical methods to solve the differential - algebraic equations, after each integral step, due to the calculation errors, the values $\mathbf{s}_k$, $\dot{\mathbf{s}}_k$ no longer satisfy the position and velocity constraint equation:

$$\mathbf{f}(\mathbf{s}_k) \neq \mathbf{0}, \dot{\mathbf{f}}(\mathbf{s}_k) \neq \mathbf{0} \qquad (k = 1, 2, ...) \tag{13}$$

Following the Baumgarte stabilization method [9-10], instead of solving the equation:

$$\ddot{\mathbf{f}} = 0 \tag{14}$$

We will proceed to solve the equation:

$$\ddot{\mathbf{f}} + 2\alpha\dot{\mathbf{f}} + \beta^2\mathbf{f} = \mathbf{0},\ \alpha > 0,\ \beta > 0 \tag{15}$$

The terms $2\alpha\dot{\mathbf{f}}, \beta^2\mathbf{f}$ play as control terms. By solving equation (15) instead of solving equation (14), we will gradually or totally eliminate the accumulated errors during the integration process.

Thus, the system of equations (12) is replaced by the following equation system:

$$\begin{bmatrix} \mathbf{M} & \boldsymbol{\Phi}_s^T \\ \boldsymbol{\Phi}_s & \mathbf{0} \end{bmatrix}\begin{bmatrix} \ddot{\mathbf{s}} \\ \boldsymbol{\lambda} \end{bmatrix} = \begin{bmatrix} \mathbf{p}_1 \\ \tilde{\mathbf{p}}_2 \end{bmatrix} \tag{16}$$

with

$$\tilde{\mathbf{p}}_2(\dot{\mathbf{s}}, \mathbf{s}) = -\dot{\boldsymbol{\Phi}}_s(\mathbf{s})\dot{\mathbf{s}} - 2\alpha\,\boldsymbol{\Phi}_s(\mathbf{s})\dot{\mathbf{s}} - \beta^2\mathbf{f}(\mathbf{s}),\ \tilde{\mathbf{p}}_2(\dot{\mathbf{s}}, \mathbf{s}) \in \mathbb{R}^r \tag{17}$$

When we choose α, β as positive constants, from the system of differential equations (15) we get $\mathbf{f} \to \mathbf{0}$ when $t \to +\infty$. Then the binding conditions $\mathbf{f} = \mathbf{0}$ will be better guaranteed at each calculation step. The stability of the solutions of the system of equations (15) at each calculation step is guaranteed. At first Baumgarte chose $\alpha = 5, \beta = 5$ and found the result to be quite good. Empirically, choose α, β from 1 to 20 or $\alpha = 1/\Delta t$, $\beta = \sqrt{2}/\Delta t$ with Δt as the integral step. The Baumgarte stabilization method is generally simple and highly effective. However, at the kinetic unusual values, this new method does not produce the desired results.

To eliminate Lagrangian multipliers, convert the system of differential algebraic equations (16) to the system of ordinary differential equations with the number of equations equal to the residual extrapolation coordinates of the system when repeating the content of the orthogonal theorem [1]. According to the orthogonal theorem we have the formula:

$$\boldsymbol{\Phi}_s\mathbf{R} = \mathbf{0} \text{ hay } \mathbf{R}^T\boldsymbol{\Phi}_s^T = \mathbf{0} \tag{18}$$

Where

$$\boldsymbol{\Phi}_q(\mathbf{s}) = \begin{bmatrix} \frac{\partial f_1}{\partial q_1} & \frac{\partial f_1}{\partial q_2} & \cdots & \frac{\partial f_1}{\partial q_f} \\ \vdots & \ddots & & \vdots \\ \frac{\partial f_r}{\partial q_1} & \frac{\partial f_r}{\partial q_2} & \cdots & \frac{\partial f_r}{\partial q_f} \end{bmatrix}, \boldsymbol{\Phi}_z(\mathbf{s}) = \begin{bmatrix} \frac{\partial f_1}{\partial z_1} & \frac{\partial f_1}{\partial z_2} & \cdots & \frac{\partial f_1}{\partial z_r} \\ \vdots & \ddots & & \vdots \\ \frac{\partial f_r}{\partial z_1} & \frac{\partial f_r}{\partial z_2} & \cdots & \frac{\partial f_r}{\partial z_r} \end{bmatrix} \tag{19}$$

$$\mathbf{R}(\mathbf{s}) = \begin{bmatrix} \mathbf{E} \\ -\boldsymbol{\Phi}_z^{-1}\boldsymbol{\Phi}_q \end{bmatrix} \tag{20}$$

with $\mathbf{E}$ is the unit matrix, $\mathbf{E} \in \mathbb{R}^f, \mathbf{R}(\mathbf{s}) \in \mathbb{R}^{n \times f}$ So we have:

$$\boldsymbol{\Phi}_s = \left[\boldsymbol{\Phi}_q\ \ \boldsymbol{\Phi}_z\right], \boldsymbol{\Phi}_q \in \mathbb{R}^{r \times f}, \boldsymbol{\Phi}_z \in \mathbb{R}^r \tag{21}$$

The system of equations (16) can be rewritten as follows:

$$\mathbf{M}(\mathbf{s})\ddot{\mathbf{s}} + \boldsymbol{\Phi}_s^T(\mathbf{s})\boldsymbol{\lambda} = \mathbf{p}_1(\mathbf{s}, \dot{\mathbf{s}}, t) \tag{22}$$

$$\boldsymbol{\Phi}_s(\mathbf{s})\ddot{\mathbf{s}} = \tilde{\mathbf{p}}_2(\dot{\mathbf{s}}, \mathbf{s}) \tag{23}$$

Multiply the left side of the equation (22) with the matrix $\mathbf{R}^T$ and pay attention to the orthogonality (18), the system of equations (22), (23) is transformed into the form:

$$\begin{bmatrix} \mathbf{R}^T(\mathbf{s})\mathbf{M}(\mathbf{s}) \\ \boldsymbol{\Phi}_s(\mathbf{s}) \end{bmatrix}\ddot{\mathbf{s}} = \begin{bmatrix} \mathbf{R}^T\mathbf{p}_1(\dot{\mathbf{s}}, \mathbf{s}, t) \\ \tilde{\mathbf{p}}_2(\dot{\mathbf{s}}, \mathbf{s}) \end{bmatrix} \tag{24}$$

If we include symbols:

$$\mathbf{A} = \begin{bmatrix} \mathbf{R}^T(\mathbf{s})\mathbf{M}(\mathbf{s}) \\ \mathbf{\Phi}_s(\mathbf{s}) \end{bmatrix}, \mathbf{p}(\dot{\mathbf{s}}, \mathbf{s}, t) = \begin{bmatrix} \mathbf{R}^T(\mathbf{s})(\mathbf{p}_1(\dot{\mathbf{s}}, \mathbf{s}, t) \\ \tilde{\mathbf{p}}_2(\dot{\mathbf{s}}, \mathbf{s}) \end{bmatrix} \quad (25)$$

then the system of equations (24) has the form:

$$\mathbf{A}(\mathbf{s})\ddot{\mathbf{s}} = \mathbf{p}(\dot{\mathbf{s}}, \mathbf{s}, t) \quad (26)$$

The system of equations (26) is a system of ordinary differential equations of residual extrapolation coordinates. Thus we have converted the system of differential algebraic equations (5), (6) to the system of ordinary differential equations (26). System (26) is a system of ordinary differential equations. Note that when solving this system of equations the first conditions of the dependent extrapolation coordinates must satisfy the constraint conditions. The calculation of these initial conditions is elaborated in [1].

III. MOTION EQUATION OF TWO-LINK ROBOT ARM WITH PROGRAM CONSTRAINTS

Investigate the arm movement in the vertical plane as shown in Figure 1. The arm consists of 3 movable sections with mass $m_i \;\; i = 1,2,3$ and inertia moment $I_i \;\; i = 1,2$. The dimensions of the length and position of the center are, l_1, l_2, $OC_1 = a_1$, $AC_2 = a_2$ respectively. The machine arm moves under the force of torque with torque $\bar{M}$ on section 1 and the horizontal force $\vec{F}$ acting on object C

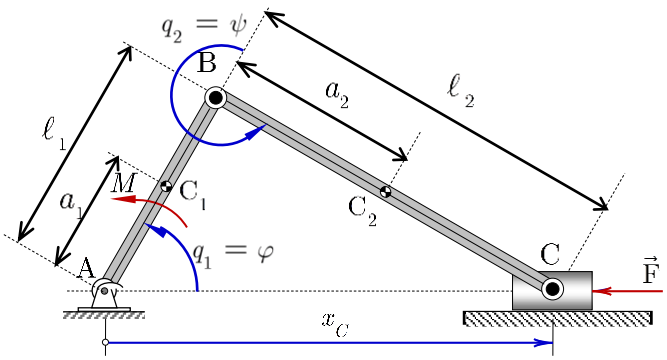

Fig. 1. Two-link robot arm

This is a closed loop multibody system with degrees of freedom of structure $f = 1$. Select 3 extrapolation coordinates $\mathbf{q} = \begin{bmatrix} q_1 & q_2 & q_3 \end{bmatrix}^T$ to determine the position of the structure. Where $q_1 = \varphi, q_2 = \psi, q_3 = x_C$. . From the figure, it is easy to set up the constraint equations:

$$f_1(\mathbf{q}) = l_1 \cos q_1 + l_2 \cos(q_1 + q_2) - q_3 = 0 \quad (27)$$

$$f_2(\mathbf{q}) = l_1 \sin q_1 + l_2 \sin(q_1 + q_2) = 0 \quad (28)$$

Kinetic energy of the mechanical arm: $T = T_1 + T_2 + T_3$

Where: $T_1 = \frac{1}{2}(I_1 + m_1 a_1^2)\dot{q}_1^2, \quad T_2 = \frac{1}{2} m_2 v_{C_2}^2 + \frac{1}{2} I_2 \omega_2^2$

$$T_2 = \frac{1}{2} m_2 \left[l_1^2 \dot{q}_1^2 + a_2^2 \dot{q}_2^2 - 2 l_1 a_2 \dot{q}_1 \dot{q}_2 \cos(q_1 - q_2) \right] + \frac{1}{2} I_2 \dot{q}_2^2$$

$$T_3 = \frac{1}{2} m_3 v_3^2 = \frac{1}{2} m_3 \dot{q}_3^2$$

From that the kinetic equation takes the form

$$T = \frac{1}{2}(I_1 + m_1 a_1^2 + m_2 l_1^2)\dot{q}_1^2 + \frac{1}{2}(I_2 + m_2 a_2^2)\dot{q}_2^2 + \frac{1}{2} m_3 \dot{q}_3^2 - m_2 l_1 a_2 \dot{q}_1 \dot{q}_2 \cos(q_1 - q_2)$$

Potential energy of structure:

$$\Pi = m_1 g a_1 \sin q_1 + m_2 g l_1 \sin q_1 - m_2 g a_2 \sin q_2$$

Virtual work of forces without potential energy:

$$\delta A = M \delta q_1 - F \delta q_3$$

The extrapolation force of the forces without potential energy:

$$Q_1^* = M, Q_2^* = 0, Q_3^* = -F$$

Replace the kinetic equation, potential energy, extrapolation and associated equations into the Lagrangian equations with multipliers.

$$\frac{d}{dt}\left(\frac{\partial T}{\partial \dot{q}_k}\right) - \frac{\partial T}{\partial q_k} = Q_k - \sum_{i=1}^{2} \lambda_i \frac{\partial f_i}{\partial q_k}, \quad k = 1,2,3$$

We infer the system of movemenet equations of the structure:

$$\begin{aligned} &(I_1 + m_1 a_1^2 + m_2 l_1^2)\ddot{q}_1 - m_2 l_1 a_2 \ddot{q}_2 \cos(q_1 - q_2) \\ &- m_2 l_1 a_2 \dot{q}_2^2 \sin(q_1 - q_2) + (m_1 a_1 + m_2 l_1) g \cos q_1 \\ &= M + \lambda_1 (l_1 \sin q_1 + l_2 \sin(q_1 + q_2)) \\ &- \lambda_2 (l_1 \cos q_1 + l_2 \cos(q_1 + q_2)) \end{aligned} \quad (29)$$

$$\begin{aligned} &- m_2 l_1 a_2 \ddot{q}_1 \cos(q_1 - q_2) + (I_2 + m_2 a_2^2)\ddot{q}_2 \\ &+ m_2 l_1 a_2 \dot{q}_1^2 \sin(q_1 - q_2) - m_2 g a_2 \cos q_2 \\ &= \lambda_1 l_2 \sin(q_1 + q_2) - \lambda_2 l_2 \cos(q_1 + q_2) \end{aligned} \quad (30)$$

$$m_3 \ddot{q}_3 = -F + \lambda_1 \quad (31)$$

The differential equations (29), (30), (31) and nonlinear algebraic equations (27), (28) form the system of Differential Algebraic Equations describing the motion of a two-link robot arm with program constraints.

IV. NUMERICAL SIMULATION

The differential - algebraic equations (27) to (31) we can rewrite in matrix form (12). From there, eliminate the Lagrangian multipliers to obtain a system of 3 nonlinear differential equations (26). Then use MATLAB software to solve the system of non-linear differential equations of the system. To study numerical simulation, we choose the parameters of geometry and mass of machine arm according to the document [2] and record in Table 1.

Table 1. Geometric and mass parameters of a robot arm

Section	length ℓ_i $[m]$	Centering block position a_i $[m]$	Mass $[kg]$	Inertia Moment of the mass opposite Centering block $[kgm^2]$
1	2	0	200	450
2	3.5	1.75	35	35
3			25	

Besides, [2]

- Active torque:

$$M = 41,450 + 0.01\sin(\Omega t)\left[Nm\right],\ \ \Omega = 2\pi\left[rad/s\right]$$

- The force exerted F is a function of the velocity and position of the last section C:

+ When $\dot{x}_C > 0$,

$$F = \begin{cases} -\dfrac{282,857}{6 - x_C} + 62,857 & if \quad 1.5 \le x_C \le 5 \\ -110,000\left[1 - \sin 2\pi\ \ x_C - 5.25\right] & if \quad 5 \le x_C \le 5.5 \end{cases}$$

+ When $\dot{x}_C \le 0$ then $F = 0$.

Next, we present a number of numerical simulation research results, using MATLAB software.

Case 1: $\varphi_0 = \pi\left[rad\right], \dot{\varphi}_0 = 1\left[rad/s\right]$

Using the constraint equations (27) and (28) we determine the initial conditions of the dependent coordinates $\psi(0),\ \dot{\psi}(0),\ x_C(0), \dot{x}_C(0)$. The numerical simulation results using MATLAB software are presented in Figures 3 and 4. In which Figure 3 is the graph of the $\varphi(t)$ rotation angle of the driving section AB, the $\psi(t)$ swing angle of the connection section BC and the angular velocity of $\dot{\varphi}(t), \dot{\psi}(t)$. Figure 4 shows the rule of motion and velocity of slider C. From Figure 3, we see that the driving section AB of the mechanism does not rotate the whole circle.

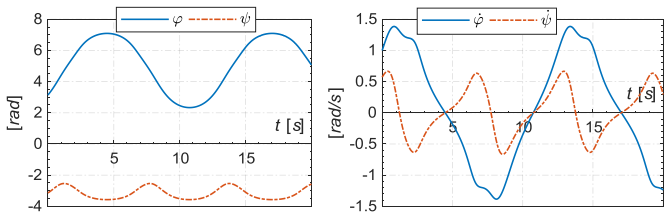

Fig. 3. Motion chart of the sections

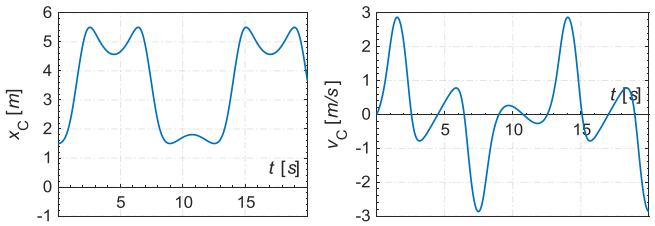

Fig. 4. Motion chart of the slider

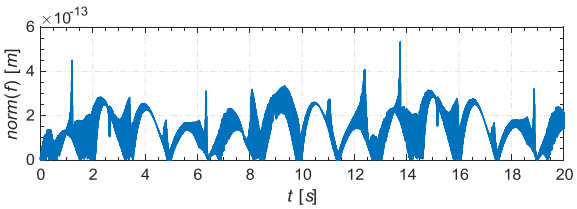

Fig. 5. Constraint equation

Figure 5 shows the accuracy of the result calculated using the graph of equation

$$\left|f\right| = \sqrt{f_1^2 + f_2^2} \tag{32}$$

Case 2: $\varphi_0 = \dfrac{\pi}{2}\left[rad\right], \dot{\varphi}_0 = 1\left[rad/s\right]$

The numerical simulation is similar to the case 1. Using the constraint equations (27) and (28) we determine the initial conditions of dependent coordinates $\psi(0),\ \dot{\psi}(0),\ x_C(0), \dot{x}_C(0)$. The numerical simulation results using MATLAB software are presented in Figures 6 and 7. Where Figure 6 is a graph of the rotation angle $\varphi(t)$ of the driving section AB, the swing angle $\psi(t)$ of the connection section BC and their angular velocity $\dot{\varphi}(t), \dot{\psi}(t)$. Figure 7 shows the laws of motion and the velocity of slider C. From Figure 6, we can see that the driving section AB rotates the whole circle.

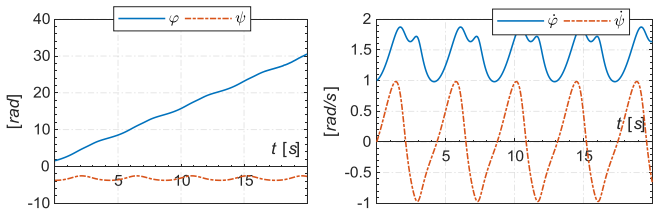

Fig. 6.. Motion chart of the sections

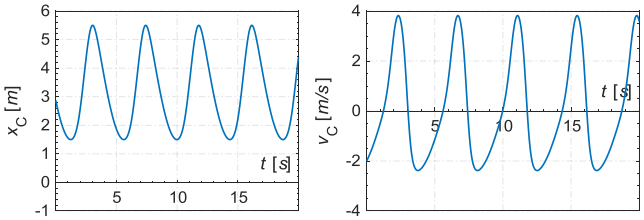

Fig. 7. Movement graph of the slider

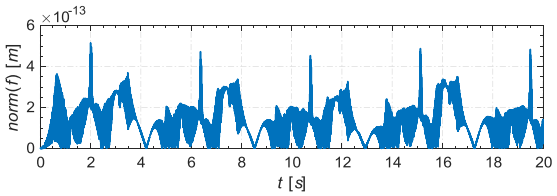

Fig. 8. Constrain t equations

Figure 8 shows the accuracy of the results calculated using the graph of the quadratic standard of the two constraint equations calculated according to formula (32).

Case 3 : $\varphi_0 = \pi\left[rad\right], \dot{\varphi}_0 = 0.5\left[rad/s\right]$

The numerical simulation is similar to the case 1. Using the constraint equations (27) and (28) we determine the initial conditions of the dependent coordinates $\psi(0)$, $\dot{\psi}(0)$, $x_C(0), \dot{x}_C(0)$.. The numerical simulation results by MATLAB software are presented in Figures 9 and 10. Where Figure 9 is a graph of the rotation angle $\varphi(t)$ of the driving section AB, the swing angle $\psi(t)$ of the connection section BC and their angular velocity $\dot{\varphi}(t), \dot{\psi}(t)$. Figure 10 shows the laws of motion and velocity of slider C. From Figure 9, we can see that the driving section AB of the device does not rotate the whole circle

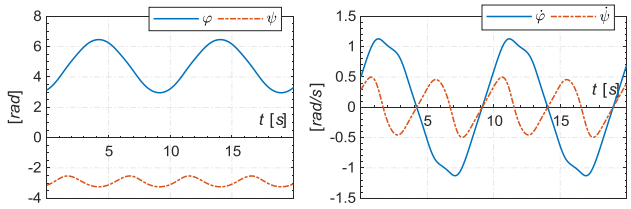

Fig. 9. Motion chart of the sections

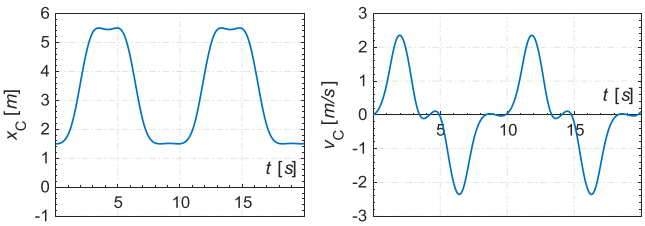

Fig. 10. Movement graph of the slider

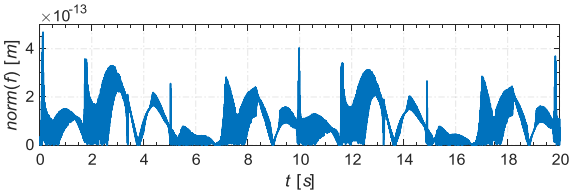

Fig. 11. Constraint equation

Figure 11 shows the accuracy of the results calculated using the graph of the quadratic standard of the two constraint equations calculated according to formula (32).

Case 4: $\varphi_0 = \pi\left[rad\right], \dot{\varphi}_0 = 1.5\left[rad/s\right]$

The numerical simulation is similar to the case 1. Using the constraint equations (27) and (28) we determine the initial conditions of the dependent coordinates $\psi(0)$, $\dot{\psi}(0)$, $x_C(0), \dot{x}_C(0)$.. The numerical simulation results by MATLAB software are presented in Figures 12 and 13. Where Figure 12 is a graph of the rotation angle $\varphi(t)$ of the driving section AB, the swing angle $\psi(t)$ of the connection section BC and their angular velocity $\dot{\varphi}(t), \dot{\psi}(t)$. Figure 13 shows the laws of motion and velocity of slider C. From Figure 12, we can see that the driving section AB of the device rotates the whole circle.

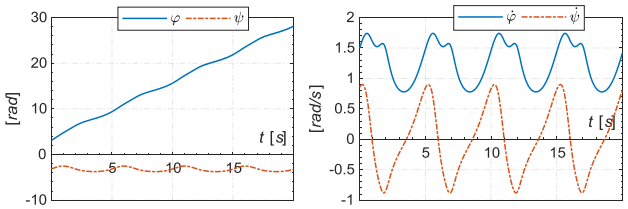

Fig. 12. Motion diagram of the sections

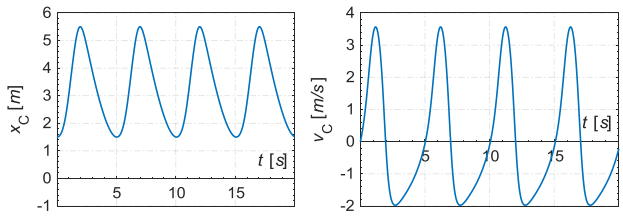

Fig. 13. Movement graph of the slider

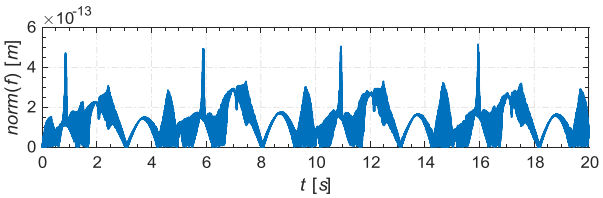

Fig.14. Constraint equation

Figure 14 shows the accuracy of the results calculated using the graph of the quadratic standard of the two constraint equations calculated according to formula (32).

V. CONCLUSION

The differential equations that describe the motion of the robotic arm with a program constraint are generally strong nonlinear differential equations. As known in nonlinear dynamics, the solutions of these equations depend on the catchment basin. In this paper, thanks to numerical simulation techniques, we see the dependence of the movement patterns of the two-link robot manipulator on the initial conditions. The motion of the links are very different, depending on the initial conditions: the active link can rotate the full circle or just oscillate.

REFERENCES

[1] Nguyen Van Khang, "Dynamics of Multibody Systems (in Vietnamese)", Sciene and Technical Publishing House, Hanoi (2017).

[2] E. J. Haug, "Computer Aided Kinematics and Dynamics of Mechanical Systems, Vol.1: Basic Methods", Allyn and Bacon, Boston (1989).

[3] J. G. De Jalon, E. Bayo, "Kinematic and Dynamic Simulation of Multibody Systems", Springer-Verlag, New York (1994).

[4] W. Schiehlen, P. Eberhard,"Applied Dynamics", Springer-Verlag, Berlin (2014).

[5] T. R. Kane, D. A. Levinson, "Dynamics/ Theory and Applications", McGraw-Hill, New York (1985).

[6] Nguyen Van Khang, "Kronecker product and a new matrix form of Lagrange equations with multipliers for constrained multibody systems", Mechanics Research Communications 38 (2011), pp. 294-299.

[7] W. Schiehlen (Editor), "Nonlinear Dynamics in Engineering Systems", Springer, Berlin (1989).

[8] S. H. Strogatz, "Nonlinear Dynamics and Chaos", Westview Press (2000).

[9] J. Baumgarte, "Stabilization of constraints and integrals of motion in dynamic systems", Computer Methods in Applied Mechanics and Engineering, 1 (1972), pp. 1-16.